



Characteristics of kinetic, thermodynamic and design equations for the analysis of nickel and zinc sorption onto impregnated activated carbon

W.F. Zaher^a, A.M.M. Eltorky^b, O.A. Abdel Moamen^{a,*}

^aHot Laboratories Center, Atomic Energy Authority of Egypt, Cairo, Egypt, Tel. +201001336124; Fax: +20244620772; emails: eng-olaa@hotmail.com (O.A. Abdel Moamen), walaa_fawzy@yahoo.com (W.F. Zaher)

^bFaculty of Science, Zagazig University, Zagazig, Egypt, email: a.torky58@yahoo.com

Received 1 May 2017; Accepted 5 December 2017

ABSTRACT

The sorptive removal of Ni(II) and Zn(II) cations from aqueous solution using synthesized nano-sized impregnated activated carbon (IAC) prepared from rice husk (RH) was scrutinized. The sorbent was synthesized via a chemical activation technique using phosphoric acid. The influence of initial cation concentration and solution pH on the sorption of Zn(II) and Ni(II) cations was studied. The kinetic data have been analyzed via the use of a pseudo-first-order and pseudo-second-order models and KASRA equation. The experimental data were described better by the pseudo-second-order kinetic equation and KASRA model. Equilibrium sorption isotherms and sorption rate studies were examined. The experimental data were evaluated by Langmuir, Langmuir-dual site, Dubinin–Radushkevich and Redlich–Peterson sorption models. The Langmuir-dual site parameters were calculated from the Langmuir equation that assumes the presence of two sorbent sites of different nature. Rooted in the dimensionless separation factor, it was deduced that the concerned cations sorption mechanism in type I sites was chemical sorption, while in the case of type II sites it was a physical sorption. The sorption of Zn(II) and Ni(II) process onto IAC occurred spontaneously, in an exothermic nature, and with increased randomness.

Keywords: Nano-sized impregnated activated carbon; Sorption; Zn(II); Ni(II); Mechanism

1. Introduction

Discharge of poorly treated or untreated wastewater containing poisonous heavy metals for instance Cd, Cr, Ni, Cu, Zn and Pb from industrial effluents onto natural water bodies is a chief environmental problem owing to their high poisoning, non-biodegradability and their tendency to build-up through the food chain [1]. Ni(II) and Zn(II) cations are amid these metals which are utilized most often in industries to manufacture metallic alloys, stainless steel, chargeable batteries, coins, casting and metallurgy. They can be entered onto the environment throughout the natural ways and human activities which cause pollution in the environment [2,3]. Trace concentrations of Ni(II) and Zn(II) cations

are very significant in physiological activities of living tissues as well as controlling biochemical processes. Conversely, in high cation concentration they can cause problems in humans such as skin burn, stomach pain, cancer, asthma, cardiopulmonary disorders, brain damage, chronic bronchitis, etc. [4].

Owing to health concerns, World Health Organization has recommended guidelines for these two metals for drinking water as 0.02 and 3 mg/L, respectively [5,6]. Thus, the removal of those cations from wastewater is tremendously significant before their discharge into the aquatic system. Conventional treatment technologies have been widened to remove Ni(II) and Zn(II) cations from contaminated water including ion exchange, chemical precipitation, membrane separation, electrocoagulation, nanoparticles, dialysis/electrodialysis

* Corresponding author.

and sorption/filtration [7–10]. Operational and capital costs frequently limit the effectiveness of these methods, mainly, when large effluents volumes enclose relatively low cations concentrations [10]. On the contrary, the sorption method is an extremely effective technique since it is a cost-effective and simple process for eliminating heavy metals from dilute solutions [11]. Lately, a diversity of cheap materials have been tested as sorbents for Ni(II) and Zn(II) removal from aqueous solution in order to find cheaper alternatives for the conventional expensive sorbents [12]. Activated carbons (ACs) act as efficient sorbents owing to their porosity, high loading capacity and well sophisticated internal surface area [13]. The commercially accessible ACs are considered costly as a result of using a high starting materials cost involved in manufacturing them and thus, there is an increased concern in using readily available and cheap materials as precursors for the preparation of AC. In this concern, a broad variety of industrial and agricultural wastes are commonly used as starting materials, for instance peach stones [14], saw dust [15], bamboo bark [16], rice husk (RH) [17], etc. RH is one of the most significant agricultural residues in quantity as it represents annually about 500 million tons in developing countries, roughly 100 million RH tons are available yearly for utilization in those countries only [17]. It can be considered as an economical and highly accessible material, in addition being renewable, which are advantageous characteristics for their use as precursors of cost-effective ACs from environmental and economic aspects. The activation of AC via the use of phosphoric acid had been paid more attention owing to simple operation, low energy and less pollution [18]. The main aim of this study is to convert RH to useful and valuable sorbent and assessment of the sorption potential of this sorbent for Ni(II) and Zn(II) removal from aqueous solution. The nano-sized AC employed in this work was prepared from RH by chemical activation via the use of phosphoric acid as a dehydrating agent, and the synthesized impregnated activated carbon (IAC) was analyzed by X-ray diffraction (XRD), Fourier transformed infrared spectroscopy (FTIR), thermo-gravimetric analysis (TGA), surface measurements and surface morphological properties.

The produced IAC was used for the removal of Ni(II) and Zn(II) cations from aqueous solutions by sorption. The influence of several parameters such as initial pH, initial cation concentration, sorbent dose and contact time on the loading capacity is examined. The equilibrium and dynamic rate data of the sorption process were afterward analyzed to study the sorption kinetics, isotherms and sorption mechanism of Ni(II) and Zn(II) cations onto the prepared nano IAC. The amount of sorbent required to determine the quantity of contaminated water to be treated was proposed.

2. Experimental section

2.1. Materials

All chemicals utilized in this work were of analytical grade. Phosphoric acid (99%) was purchased from Merck, Germany. Ni(II) and Zn(II) chlorides (>99%) were purchased from Sigma-Aldrich Co.

2.2. Synthesis of nano impregnated activated carbon

Rooted in the main purpose of this study, RH, as a precursor, was gathered from the local market. To produce AC, Primarily, RH was washed thoroughly with bi-distilled water to get rid of any impurities and adhering dust. After that, the drying process at about 110°C for 1 h was carried out. The dried RH was ground into fine powders before the activation process. Then, RH was heated at about 400°C for 2 h under the nitrogen protection to acquire a carbonized rice husk (CRH). The CRH was impregnated with about 85% wt. phosphoric acid for 24 h at impregnation ratio of 2:1 (volume mL of acid/mass g of RH). The activation reaction was employed at a temperature of about 400°C and maintained for 4 h. The product was thoroughly washed with hot distilled water to eliminate excess phosphorus compounds. Washing was repeated until the pH of filtrate (yielded from washing process) reaches 7. The gathered filtrate from the washing process of the activated RH was basified via the use of NaOH to reach pH = 7 under continuous stirring. Afterward, the precipitate was filtrated, washed and dried at 110°C for 12 h to attain impregnated nano-sized AC ready for sorption test. The trial experiments demonstrated that the used conditions give superior IAC in term of suitable surface properties and yield. The synthesis procedure is illustrated in Fig. 1. The yield of RH was counted from the ratio between IAC and AC, where IAC is the impregnated activated carbon mass (g) and AC is the raw activated carbon sample mass (g). The AC preparation experiments were achieved several times to achieve satisfactory IAC samples for further characterization and analysis. Accordingly, the % yield is an average value of all the sufficient experiments.

2.3. Preparation of stock solution

The stock solution of Ni(II) and Zn(II) cations with initial concentration of 100 mg/L was prepared by serial dilution of 1,000 mg/L solution. Solvents (1.0 M hydrochloric acid and 1.0 M sodium hydroxide) were employed to adjust the pH value of the stock solution.

2.4. IAC characterization

2.4.1. X-ray diffraction analysis

XRD was executed on IAC so as to determine the amorphous or crystallinity nature of the sample. The analysis was executed using CuK α radiation by Shimadzu X-ray diffractometer – 6000 series, Germany.

2.4.2. Thermo-gravimetric analysis

The TGA analysis was carried out to study the thermal behavior of the synthesized material with a heating rate of 10°C/min via TGA-60A, Shimadzu, Japan.

2.4.3. Fourier transform infrared spectroscopy

FTIR analysis was used to estimate the sample surface functional groups by means of BX-1-America spectrometer with a frequency range of 4,000–400 cm⁻¹.

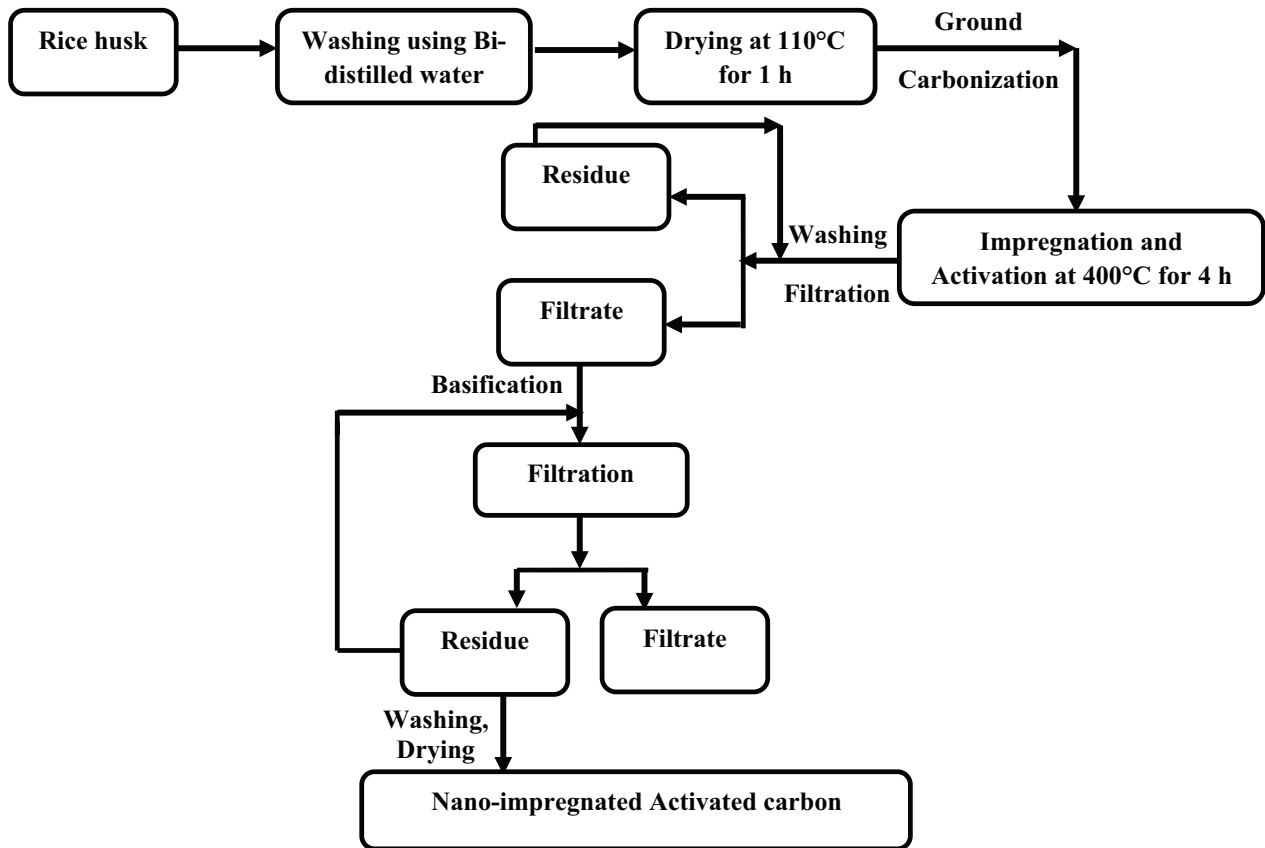


Fig. 1. Scheme for the preparation of the synthesized nano impregnated activated carbon.

2.4.4. Transmission electron microscopy

Transmission electron microscopy (TEM) is a vital characterization technique for directly imaging nano-sized materials to acquire quantitative measures of particles and sample morphology. The TEM nano-graph was executed using JEM 1000CX, JEOL, Japan.

2.4.5. Surface area analysis

The surface area of the AC before and after impregnation was determined using BET method, at which nitrogen adsorption isotherm was quantified by a fully automated surface area analyzer (Nova Instrument, Quantachrome Corporation, USA).

2.4.6. Point of zero charge (pH_{zpc}) of AC and IAC

The zero point of charge (pH_{zpc}) of AC and IAC was determined following the well known salt addition method reported in literature [19]. The difference between final and initial pH (ΔpH) was plotted against initial pH (pHi) (Fig. 3(E)). The pH value where net surface charge was zero is considered to be the zero point of charge (pH_{zpc}) of the material.

2.5. Batch sorption studies

Batch sorption experiments were carried out at ambient temperature to study the influence of pH, sorbent dosage and

contact time on the sorption efficiency of Ni(II) and Zn(II) cations by the IAC. The experiments were performed in triplicates and the average values were presented. Experiments were performed in Erlenmeyer flasks and the concentration of the residual Ni(II) and Zn(II) cations was measured using atomic absorption spectroscopy (Buck Scientific model VGP 210). The loading capacity (q_e) and elimination efficiency (%E) of Ni(II) and Zn(II) were estimated using the subsequent equations [19]:

$$q_e = (C_o - C_e) \cdot V/m \quad (1)$$

$$\%E = \frac{(C_o - C_e)}{C_o} \times 100 \quad (2)$$

where C_o and C_e are the initial and equilibrium concentration of cations (mg/L), V is the total solution volume (L) and m is the weight (g) of IAC.

Kinetic studies were executed by taking 400 mg of synthetic IAC in 50 mL of aqueous solution containing known concentration of metal ion (100 mg/L for each metal ion) and neutral pH value under constant shaking using thermostatic shaker. A constant volume (2 mL) of the aliquot was withdrawn at predetermined intervals time while the solution was being continuously shaken, consequently the ratio of the solution volume to the IAC weight ratio does not vary from its initial value. The withdrawn aliquot was centrifuged

to detach the solid from the liquid phase, and the sorbed cations amount at any time, q_t (mg/g), was calculated as follows:

$$q_t = (C_o - C_t) \cdot V/m \quad (3)$$

where C_t is the time variant concentrations of Ni(II) and Zn(II) cations (mg/L).

2.6. Models for sorption kinetics

The kinetic data of Ni(II) and Zn(II) sorption were treated with pseudo-first-order and pseudo-second-order models. The non-linear form of pseudo-first-order (Eq. (5)) and pseudo-second-order (Eq. (4)) models could be expressed as follows [20,21]:

$$q_t = \frac{(K_2 q_e^2 \cdot t)}{(1 + K_2 q_e \cdot t)} \quad (4)$$

$$q_t = q_e (1 - e^{-k_1 t}) \quad (5)$$

where k_1 (min^{-1}) and k_2 ($\text{g.mg}^{-1}.\text{min}^{-1}$) are the pseudo-first-order and pseudo-second-order rate constants, respectively.

So as to explore in detail the kinetics of sorption process, a model of “kinetics of sorption study in the regions with constant sorption acceleration” (KASRA) was employed [21]. The KASRA model is rooted in the subsequent assumptions: (A) each time ranges which sorption acceleration is constant, denominated as a “region”; (B) mainly there are two regions before reaching a plateau region; (C) the boundaries amid the regions are determined via the KASRA model as follows:

$$q_t = At^2 + Bt + C \quad (6)$$

where $A = 0.5a_i$; $B = v_i - a_i t_{oi}$; $C = q_{oi} - 0.5a_i t_{oi}^2 - B t_{oi}$. a_i is the sorption kinetic acceleration in the i th region and $i = 1-3$, t_{oi} and v_{oi} are the time and velocity values in the beginning i th region, respectively, q_{oi} is the q_t value in the i th region beginning.

2.7. Models for sorption isotherms

For isotherm modeling studies, Langmuir; Langmuir-dual site; Dubinin–Radushkevich (D–R) and Redlich–Peterson (R–P) models are considered. The Langmuir isotherm model assumes a mono-layer sorption from the homogenous surface with similar heat distribution on the sorbent surface. The Langmuir-dual site isotherm assumed that the total loading capacity (Q) may be determined by the summation of sorption capacities attained from the first Q_1 and second Q_2 type of sites [11].

D–R isotherm model depicts sorption on a single type of uniform pores. In this respect, the D–R isotherm is an analogue of Langmuir type but it is more general as it does not assume a homogeneous surface or constant sorption potential. R–P model seeks to depict the degree of sorbent surface heterogeneity and the sorption sites number having the same sorption potential. The Langmuir, Langmuir-dual site, D–R

and R–P models can be mathematically expressed by the following equations, respectively:

$$q_e = \frac{Q^0 b C_e}{1 + b C_e} \quad (7)$$

$$q_e = \sum_{j=1}^N Q_{m,j} \frac{b_j C_e}{1 + b_j C_e} \quad (8)$$

$$q_e = q_m \exp(-\beta(\epsilon)^2) = q_m \exp(-\beta(RT \ln(1 + 1/C_e))^2) \quad (9)$$

$$q_e = \frac{K_R C_e}{1 + \alpha_R C_e^\beta} \quad (10)$$

where Q is the saturation capacity, b ; b_j and K_R are the equilibrium constants of Langmuir, dual-site Langmuir of site j ; q_m is the maximum sorption capacity, β is the activity coefficient related to mean sorption energy, ϵ is the Polanyi potential for D–R model and α , β are the R–P parameters models, respectively. All non-linear kinetic and isotherm equations were fitted to experimental data using the ORIGIN 6.01 software.

3. Results and discussions

3.1. Characterization

The XRD analysis (Fig. 2(A)) illustrates an amorphous structure or poorly crystallized IAC, which is a beneficial property for well-defined sorbents, with three sharp peaks at 24.39; 23.83 and 26.91 that may be owing to the disordered stacks of hexagonal graphite layers and calcium phosphosilicate ($\text{Ca}_7\text{Si}_2\text{P}_2\text{O}_{16}$) formation [20].

The TGA profile demonstrates three-step weight loss. The first was scrutinized at less than 150°C amounting to about 5% of the weight loss. This largely account for the removal of water molecules present in the sample as illustrated in Fig. 2(B). The sample was examined to be almost stable at 150°C–300°C temperature range and representing about 5% weight loss. Subsequently, significant weight loss was observed amid 300°C–400°C that signify about 50% of the weight loss. This is usually owing to cellulose and hemicelluloses decomposition. At about 400°C, percentage weight loss was showed to be comparatively small which is owing to the decomposition of lignin component that gradually degrades over a broad range of temperature, therefore yield was observed to be approximately stable.

The FTIR analysis before and after impregnation in Fig. 2(C) demonstrates the existence of peaks around 3,000–3,700 cm^{-1} which is mainly characteristic of hydrogen bond stretching vibration band (–O–H) in phenols, alcohols, carboxyl and the absorbed water from IAC. Peak at 2,883 cm^{-1} (after impregnation) signifies –C–H asymmetric or symmetric stretching vibration in aliphatic series. The band region of 1,300–900 cm^{-1} could be attributed to P=O, O–C bond in P–O–C linkage or P=OOH bond. This signifies the existence of phosphorous-oxy-containing group in the AC implying that phosphates traces stay in the carbon even after repeated

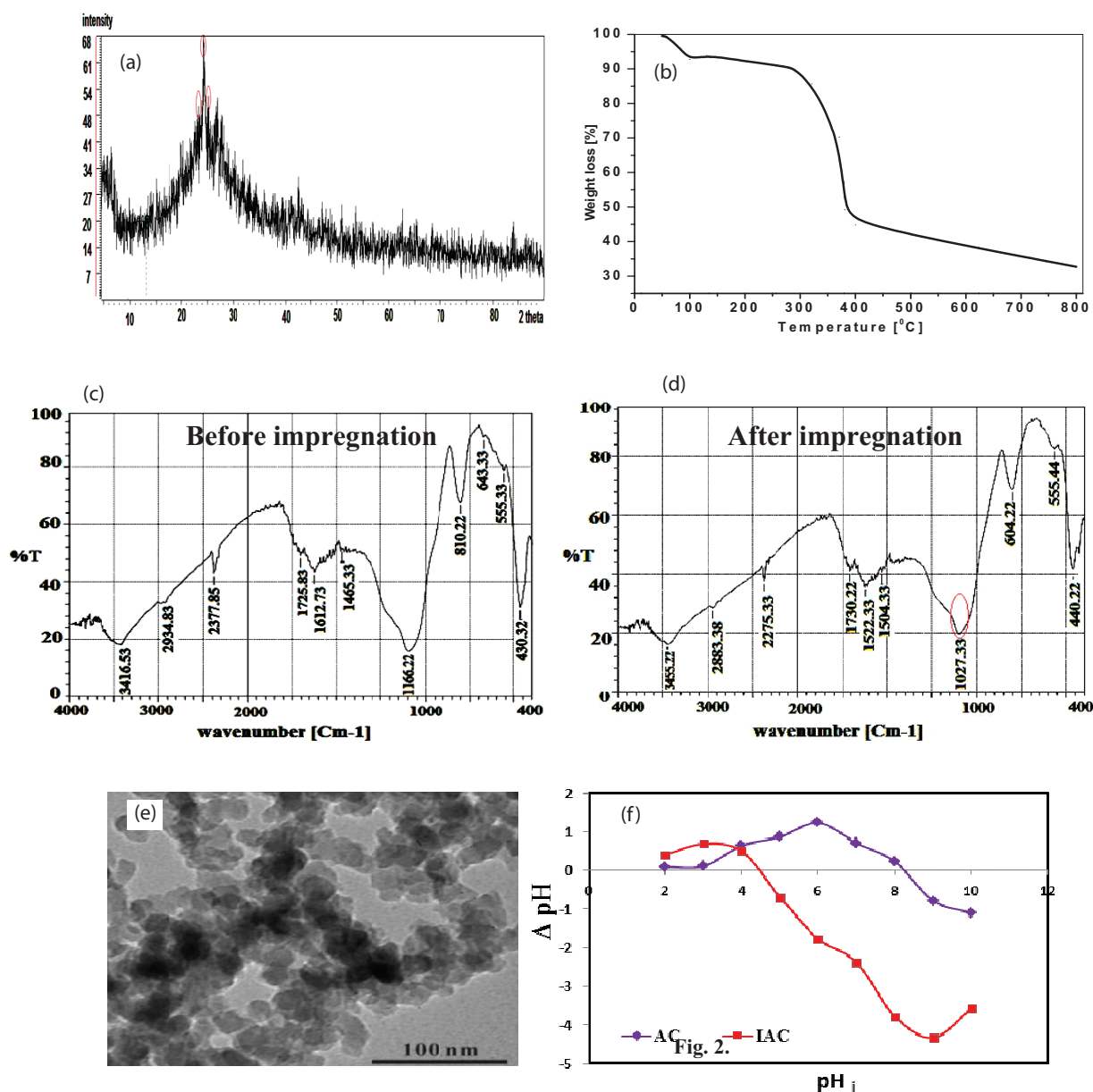


Fig. 2. Characterization of the synthesized material using (A) XRD spectroscopy analysis; (B) TGA; (C) FTIR analysis; (D) TEM nanograph and (E) pH of zero point of charge (pH_{ZPC}) for AC and IAC.

washing. Therefore, in comparison, the shift in broad band to $1,027\text{ cm}^{-1}$ could be assigned to C–O stretching in IAC. Simultaneously, it is also a characteristic of phosphorous and silica species and phosphor-carbonaceous compounds existing in the phosphoric acid-AC. The appearance of the broad band in the region $800\text{--}600\text{ cm}^{-1}$ could be assigned to O–H indicating the introduction of oxy-containing functional groups resulting from phosphoric acid [21]. The bands located at 600 and 400 cm^{-1} were assigned to the Si–O bending vibration and a symmetrical stretching vibration.

The TEM nano-graph (Fig. 2(D)) shows that the synthesized material has lumpy uniform particle morphology with narrow particle size distribution of $30\text{--}50\text{ nm}$ and average diameter of about 38 nm that refers to uniform particles growth during preparation. The exceeding results showed

that the IAC is nano-sized and sphere-like shaped with a certain degree of agglomeration.

The surface area of the prepared AC was found to be $19.53\text{ m}^2/\text{g}$ (Table 1). It was also observed that the phosphoric acid modification of the AC increased the surface area to $104.65\text{ m}^2/\text{g}$. This increase in surface area could be attributed to the phosphoric acid impregnation and washing which lead to the removal of unorganized carbon at low temperatures thereby opening the closed pores [22,23].

Fig. 2(E) indicates that the surface of IAC is more acidic ($pH_{ZPC} = 4.25$) whereas the surface of AC is alkaline ($pH_{ZPC} = 8.12$). The lower pH_{ZPC} value renders IAC to be more suitable in the removal of Zn(II) and Ni(II). The increase in acidic character of IAC reveals that the degree of protonation is inevitably affected by impregnation. The modification further contributes

Table 1
Surface area analysis data of IAC

BET surface area (m ² /g) of AC	19.53
BET surface area (m ² /g) of IAC	104.65
Average pore radius (nm)	12.54
Total pore volume (cm ³ /g)	0.1229

to the generation of weak acidic functional groups. At pH values below pH_{ZPC} , the IAC surface is positively charged while at pH above pH_{ZPC} the surface of IAC is negatively charged. At lower pH values (pH 2 and 3) the surface of IAC undergoes surface protonation due to the frequent interaction and accumulation of H⁺ ions from the bulk, which have the tendency to surround the surface of the sorbent. Besides that, the IAC surface is assumed to release the basic OH⁻ ions into the bulk which results in a slight increase in the final pH of the suspension. Hence, this results in an overall positively charged IAC surface at lower pH values (below pH_{ZPC}). However, at alkaline pH (or above the pH_{ZPC} of IAC), the surface of IAC was found to be negatively charged. Generally, with the increase in initial pH of the system, the excessive amount of OH⁻ ions in the bulk solution are counter balanced by the H⁺ ions liberated from the IAC surface. Moreover, the deprotonation of IAC results in the decrease in the final pH of the suspension and creates an overall negative charge on the IAC surface [22].

3.2. Sorption of Ni(II) and Zn(II) from aqueous solution

3.2.1. Descriptive model of metal binding by IAC as a function of pH

The sorption of Ni(II) and Zn(II) cations is extremely affected by the solution pH value as the functional group activity and sorbent surface charge could vary with the changing in the solution pH value [24]. The relation between the sorption of cations and the released protons can be acquired by linearization of a general overall mass action expression for metal sorption neglecting activity coefficients, including adsorption, hydrolysis and exchange reactions as follows [25]:

$$\log\left(\frac{[-SM]}{[S] \cdot [M]}\right) = \psi pH + \log(Kc) \quad (11)$$

where $[-SM]$ is the sorbed species concentration, $[S]$ is the sorbent vacant sites concentration, ψ is the proton coefficient, $[M]$ is the total metal species concentration in solution and Kc is the overall equilibrium constant. If Kc is independent of the pH value, then the ψ value, obtained from a linear graph of $\log([SM]/[M])$ vs. pH (Kurbatov plot) refers to the overall proton stoichiometry of the sorption equilibrium process [26] (Fig. 3(A)).

Rooted in the experimental results, it was showed that ψ value is inferior to 1 and closing to 0 illustrating that the concerned cations is not necessarily adsorbed onto the IAC in a one-to-one correspondence amid the released hydrogen ion from the sorbent and the cation loading. In other words, it is possible to propose that there would be no release of H⁺ in the process and both the concerned cations species will be adsorbed via the formation of surface complex between the sorbent surface and the concerned cations. In the second

region, with the higher degree of metallic ion hydrolysis, the specific sorption of MOH species via precipitation is likely to have become the dominant mechanism which refers to the changes in the mechanism [25,26]. The log (Kc) values varied from 2.94 to 2.75 and 2.84 to 2.62 for Zn(II) and Ni(II), respectively. This shows a larger affinity of Zn(II) than Ni(II) with IAC binding sites.

The Ni(II) and Zn(II) elimination efficiency increased considerably with an increase in the solution pH value as at acidic medium the IAC surface was more positively charged, accordingly it was framed by hydroxonium cations besides the electrostatic repulsive force amid the concerned cations and the charged IAC surface, averting the cations from reaching the vacant sites of the IAC. Furthermore, greater ionization and solubility of the metal salts in the acidic medium could indicate competition amongst sorbed cations and the hydrogen cations at low pH values. Instead, at higher values of pH, the IAC surface became more negatively charged, which should theoretically facilitate a higher removal rate. Nevertheless, the results showed lower elimination efficiency at pH 6 and 8. This may be due to the fact that further increase into pH values caused the solution to become more milky, referring the precipitation of Zn(II) and Ni(II) cations in the form of ZnOH⁺, Zn(OH)₂ (aq), Zn₂OH⁺³, Zn(OH)³⁻ and Ni(OH)⁺, respectively. The deposition of hydroxides blocked the sorbent pores and accordingly impeded the sorption of cations. The Ni(II) and Zn(II) sorption efficiency by the IAC reached a maximum at pH of 5.0 and 6.0, respectively (Fig. 3(B)) [25].

3.2.2. Effect of IAC dosage

The solution volume (50 mL) and Zn(II) and Ni(II) cation concentrations (100 mg/L) were kept constant while the amount of IAC varied from 100 to 400 mg. It can be observed from Fig. 3(C) that the concerned cations loading capacity increased swiftly with the boost in IAC dosage till reaching a plateau at the sorbent dosage of 400 mg. The increase in sorption loading capacity could be attributed to the greater availability of the number of sorbing species on the sorbent at higher dosage of sorbent. Any further addition of the sorbent beyond this did not cause any significant change in the sorption. This may be due to overlapping of sorption sites as a result of overcrowding of sorbent particles. From the economical viewpoint, 400 mg IAC was elected as an optimum parameter.

3.2.3. Effect of contact time

Ni(II) and Zn(II) cations elimination efficiency as a function of contact time is illustrated in Fig. 3(D). The sorption efficiency of both Ni(II) and Zn(II) increased with contact time and reached equilibration after 120 min. The sorption rate of the studied ions by IAC indicated that the process is quite rapid and about 75% and 85% sorption of the equilibrium value occurred within 90 min for Ni(II) and Zn(II) cations, respectively. This can be probably due to the distribution of wide pores on the synthesized IAC. The results also clarified that the IAC exhibited fast kinetics to Zn(II) more than Ni(II) cations under the optimum experimental conditions and the elimination efficiency gradually increased with time till saturation was attained at about 120 min.

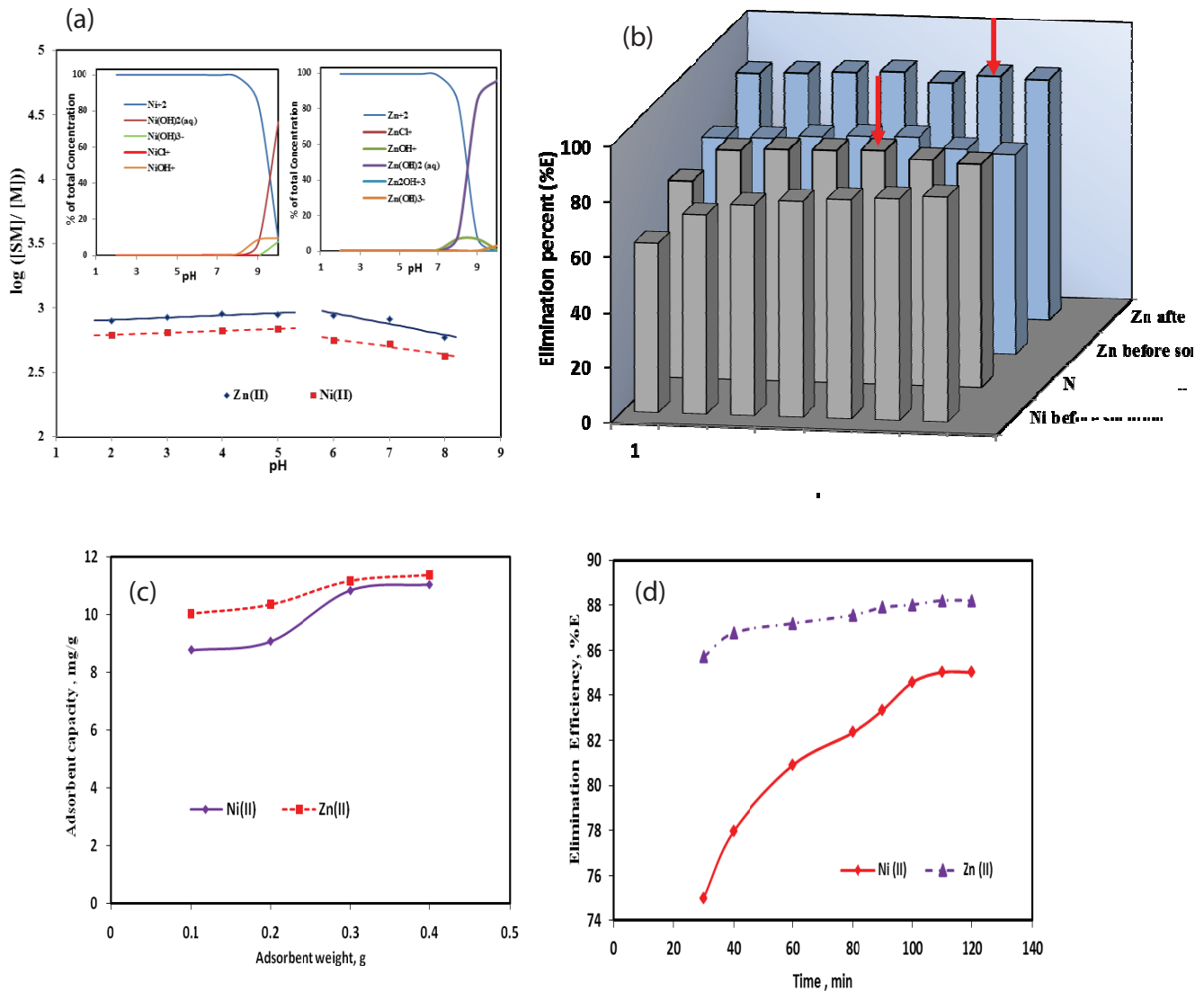


Fig. 3. (A) Influence of solution pH on the sorption removal of Zn(II) and Ni(II) cations by the synthesized IAC; (B) relation between elimination efficiency (%E) and pH value; (C) effect of sorbent dose on the removal of the concerned cations onto the sorbent and (D) effect of contact time in the evaluation of elimination efficiency.

3.2.4. Sorption kinetic models

The experimental kinetic sorption data acquired at ambient temperature (298 K) are examined using numerous kinetic models discussed above. Comparative graphs of experimental kinetic data with the above mentioned models are presented in Fig. 4(A). The acquired model parameters are listed in Table 2. It is obvious that the cations sorption demonstrated a fast initial sorption rate pursued by a relatively slow sorption. The sorption increased speedily in the first 80 min, after that, the sorption increased more quietly. The sorption equilibrium was achieved within about 90 min and the sorption kept almost steady till the end of the experiment at about 120 min. Initially, the rapid sorption could be due to the electrostatic attractions, which lead to the rapid cations transportation from solutions to the sorbent surface. The subsequent slow sorption designated

that the sorption was the domination mechanism of cations sorption [26].

The comparisons amid the utilized models were carried out via the use of Bayesian information criterion (BIC) tests and the residual error analysis (RE) (Fig. 4(B)). The BIC is used for model selection among a finite set of models. It can measure the efficiency of the parameterized model in terms of predicting the data. The RE is the difference between the observed value of the dependent variable and the predicted value.

It was found that the RE and BIC analyses of pseudo-second-order expression were lower than that of pseudo-first-order expression accordingly can be verified that the concerned cations sorption onto the IAC was governed by the pseudo-second-order kinetic model. This designated that chemical bonding amid the sorbent active sites and Ni(II) and Zn(II) cations might predominate the sorption process.

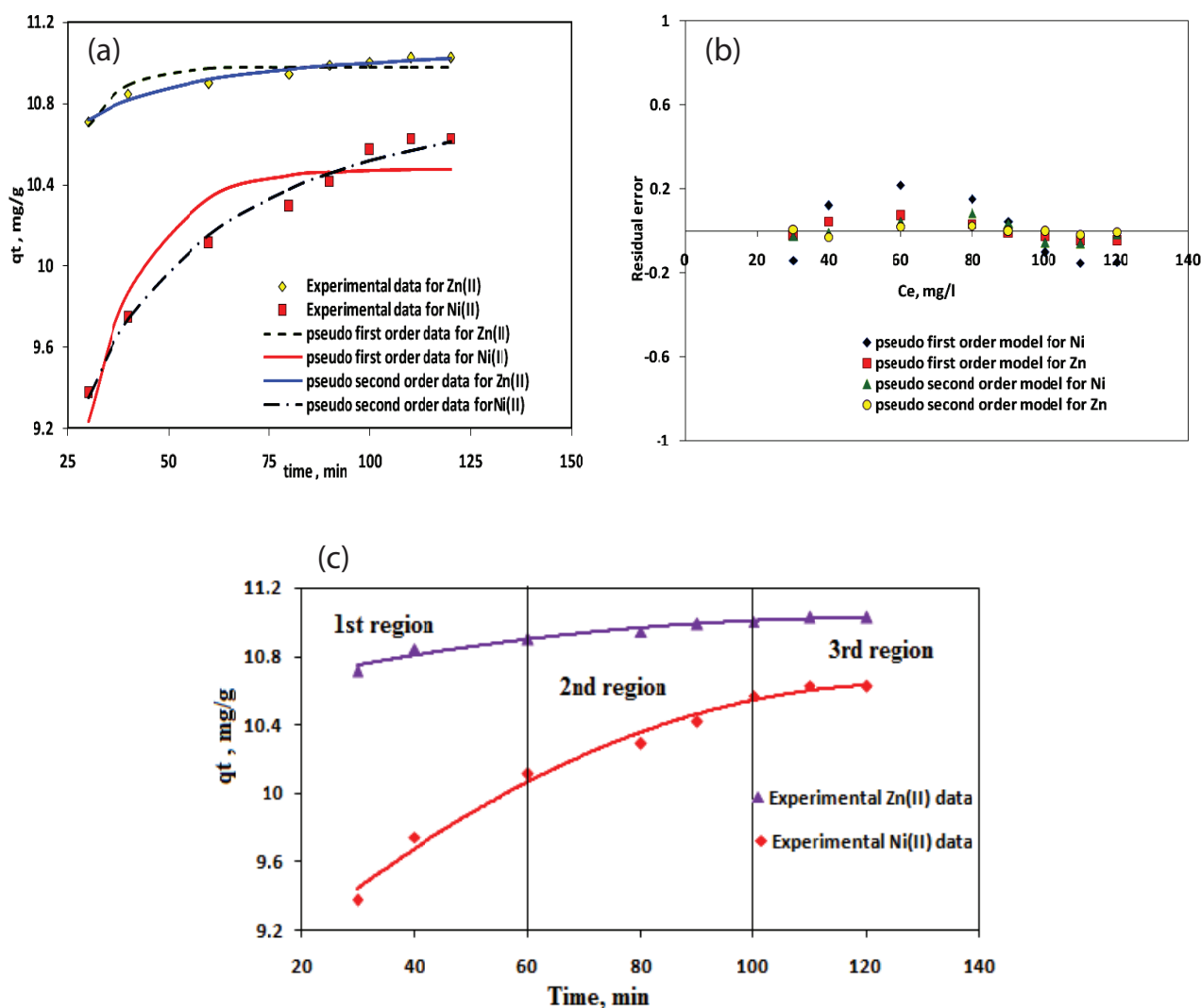


Fig. 4. (A) Non-linear kinetic behavior models for sorption of Zn(II) and Ni(II) cations onto IAC. (B) Residual error for non-linear pseudo-first-order and pseudo-second-order for Zn(II) and Ni(II) cations. (C) Schematic diagram of the sorption kinetics by the KASRA model for Zn(II) and Ni(II) cations.

From Fig. 4(C) and Table 2, it is obvious that there are two regions before reaching a plateau consistent with KASRA model which is owing to the influence of the occupied sites on the rate of sorbate sorption onto free sorption sites which is known as a braking effect. Increase in time value results in increase in the sorption of the concerned cations onto the synthesized IAC, consequently a_i was negative value and the sorption velocity value (v_i) decreased. From the first to the second region, the values of v_{oi} decreased and a_i became less negative which was owing to the decrease in the unoccupied sites number on the IAC surface. In these processes, the acceleration of sorption in both the appeared regions was negative sign and the initial sorption velocity at both the first and second regions rose with time. Finally, a plateau started at the equilibrium time.

3.2.5. Sorption equilibrium study

The sorption equilibrium studies were executed to assess the performance of the synthesized IAC for Ni(II) and Zn(II)

sorption. Non-linear Langmuir, dual-site Langmuir, D–R and R–P models are shown in Fig. 5. Consistent with Giles classification, the shape of the obtained isotherm can be ascribed to H-type (high affinity type) representing strong interaction between the concerned cations and IAC surface [27].

A plot of C_e/q_e vs. C_e for both the concerned cations showed to be linear and the aroused break-line indicated the accessibility of more than one site type for the cations described by Langmuir model [28]. The presence of two active sites types was observed from Fig. 6. In this case it is presumed that each site's type can be depicted by the Langmuir-dual site isotherm equation. The isotherm constants: Q_1 , b_1 , and Q_2 , b_2 were determined rooted in the experimental data with the use of ORIGIN (6.01) software. The Langmuir separation factor (R_L), $RL = 1/1+b \cdot C_0$, is used to assess the feasibility of sorption process, signifying when the sorption is linear ($R_L = 1$), unfavorable ($R_L > 1$), favorable ($0 < R_L < 1$) or irreversible ($R_L = 0$) [29–32].

Fig. 7 shows that the loading capacity through the site type I values for both cations were considerably higher than

Table 2
Sorption rate constant and Bayesian information criterion of pseudo-first-order, pseudo-second-order and KASRA kinetic models

Model	Parameter	Zn(II)	Ni(II)	
Pseudo-first-order	q_e , mg/g	10.98	10.48	
	K_1	0.1212	0.0710	
	BIC	0.163	0.014	
Pseudo-second-order	q_e	11.12	11.01	
	K_2	0.885	0.176	
	BIC	0.007	0.002	
KASRA 1st region	A	-0.000036	-0.00077	
	B	0.038	0.0276	
	C	9.87	9.62	
	a_1	-0.0000724	-0.00154	
	v_{o1}	0.0358	0.0032	
	q_{oi}	10.97	6.90	
	KASRA 2nd region	A	-0.000061	-0.00077
		B	0.0142	0.0276
		C	10.04	9.62
a_2		-0.000123	-0.00154	
v_{o2}		0.0043	0.0032	
q_{oi}		10.78	6.9	

the loading capacity through the site type II. The dimensionless separation factor results (R_L) indicate that its values varied significantly for the cation in reliance on the sites types. Rooted in the obtained results, it can be showed that the cations sorption on IAC type I sites was a chemical one as the R_L values are high enough and the strength of the sorption for Zn(II) cations is higher than for Ni(II) cations. Interactions amid the cations and the type II sites were a physical sorption (R_L close to zero). The plot of Langmuir separation factor (R_L) is presented in Fig. 7. The R_L values indicated the favorability of cations sorption in the studied concentration range.

The D–R plots of q_e vs. ϵ^2 for the sorption of Zn(II) and Ni(II) ions resulted in the derivation of q_m , β , E and BIC values are given in Fig. 8. From the visual analysis, the D–R isotherm expression is followed for Zn(II) and Ni(II) ions. But the values of BIC are higher than other used models, revealing that the experimental data not fitted well with the D–R isotherm model. The D–R parameters are presented in Table 3. The values of the mean free energy, E , of sorption in both cases are in the range of 8–16 kJ/mol, which are within the energy ranges of chemisorption reaction [29].

The R–P model can be used to depict the sorption equilibrium in a wide sorbate concentration range. The exponent (β) of R–P model detects the isotherm shape if β approaches to 1, the R–P model behaves consistent with Langmuir isotherm [28,29].

The β R–P parameter value was of 0.8289 and 0.8079 for Ni(II) and Zn(II) cations, respectively, signifying that the isotherm stratifies to dual-site Langmuir model better than Langmuir model. Accordingly, the isotherm modeling proposes that Ni(II) and Zn(II) sorption onto IAC correspond to physisorption and chemisorption as the values of the model parameters Q^0 and b obtained for two sites validate that cations sorption process is predominated by chemisorption as

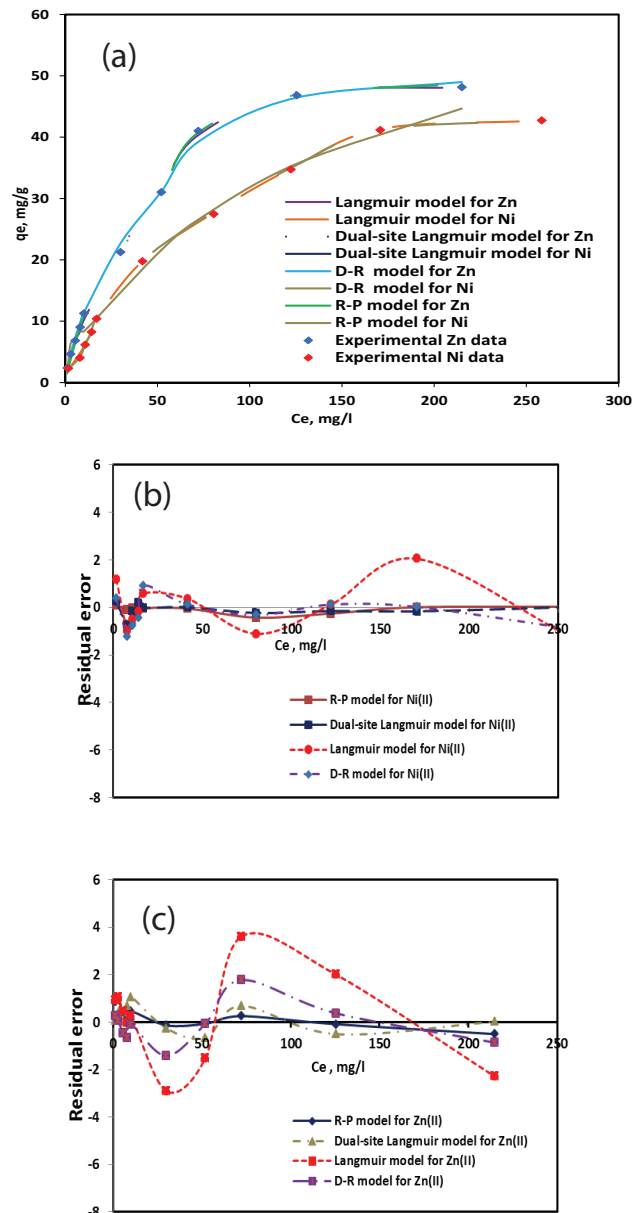


Fig. 5. (A) Equilibrium isotherm for the sorption of Zn(II) and Ni(II) cations onto synthetic IAC. Residual errors for non-linear regression of equilibrium removal data to different isotherm models for (B) Ni(II) and (C) Zn(II).

the higher values of Q_1^0 and b_1 correspond to chemisorption site while, the lower Q_2^0 and b_2 values account for physisorption site.

Thermodynamic studies are an indispensable component of predicting sorption mechanisms (e.g., chemical and physical) through estimating the thermodynamic parameters that include the Gibbs energy change (ΔG^0), the enthalpy change (ΔH^0) and the entropy change (ΔS^0). The thermodynamic parameters can be estimated according to the laws of thermodynamics as follows: $\Delta G^0 = -RT \ln(K_c) = \Delta H^0 - T\Delta S^0$ where K_c is the standard equilibrium constant that can be obtained from different ways. In 1987, Khan and Singh [33] proposed

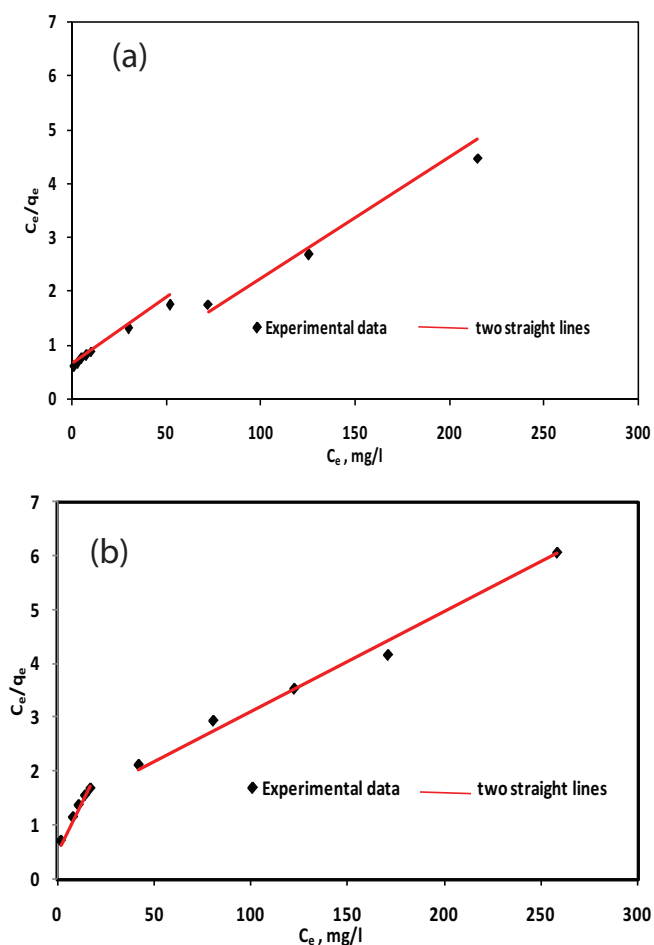


Fig. 6. A plot of C_e vs. C_e/q_e for (A) Ni(II) and (B) Zn(II) cations.

a method for calculating thermodynamic parameters rooted in the method of Biggar and Cheung [34] that uses the distribution coefficient (K_d). The K_d value can be defined as the ratio between equilibrium sorption capacity (q_e) and equilibrium concentration (C_e). In this method, K_d values are obtained by plotting $\ln(q_e/C_e)$ vs. C_e and extrapolating to zero C_e . If a straight line fits the data with a high regression coefficient (R^2), then its intersection with the vertical axis provides the value of K_d . This method has been extensively applied to calculate thermodynamic parameters. Regrettably, the units of K_d becomes L/g as C_e has units of mg/L and q_e has units of mg/g. Therefore, it is impossible to directly employ K_d for the calculation of the aforementioned parameters [34–38] as the K_c must be dimensionless. As a result, application of the distribution coefficient as it was not appropriate for calculating the thermodynamic parameters. This unit problem has been discussed by several researchers [38–40]. Taha et al. [40] suggested that the K_d (L/g) can convert into dimensionless K_c by multiplying it to a factor of 1,000 as originally proposed by Milonji [35]. The thermodynamic parameters can then be estimated as:

$$\Delta G^0 = -RT \ln(1,000K_d), \text{ then } \ln(1,000K_d) = \frac{-\Delta H^0}{R} \cdot \frac{1}{T} + \frac{\Delta S^0}{R} \quad (12)$$

The obtained thermodynamic equilibrium parameters are given in Table 4. The negative values of ΔG^0 (KJ/mol) indicate

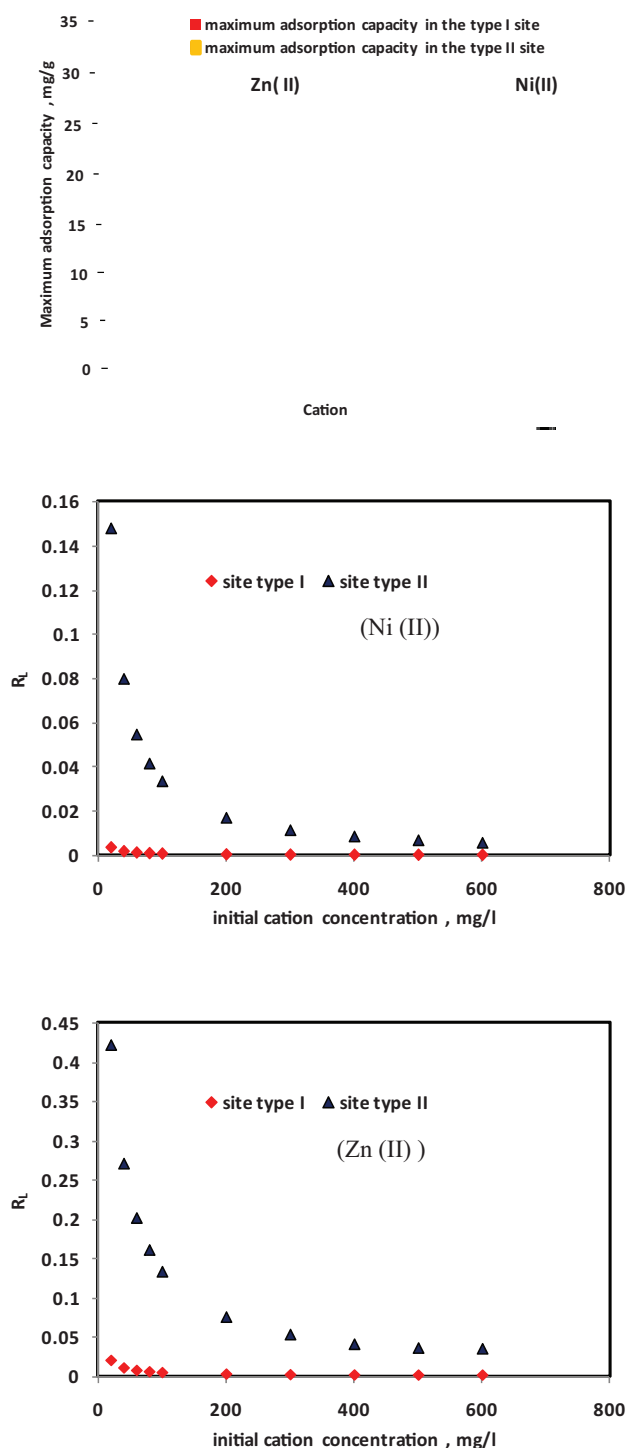


Fig. 7. Dual-site Langmuir isotherm parameters for both Ni(II) and Zn(II) cations.

the spontaneous nature of sorption of Ni(II) and Zn(II) onto IAC for the studied temperature range. Also the obtained negative values of ΔH^0 (KJ/mol) for the interval of temperatures studied (Table 4) confirms the exothermic nature of the sorption process. This exothermic phenomenon is because the total energy absorbed in bond breaking is lower than the

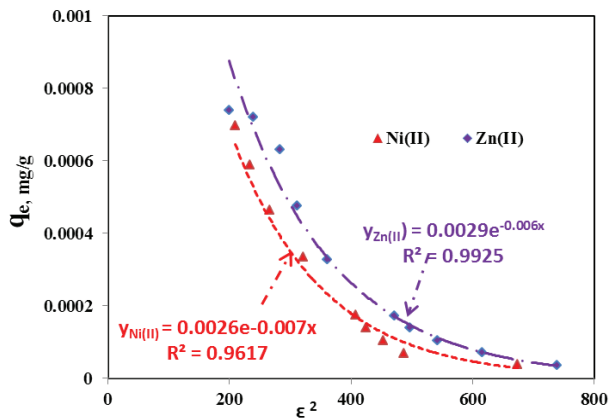


Fig. 8. D–R isotherm plots for the sorption of Ni(II) and Zn(II) cations from aqueous solutions onto synthesized IAC.

Table 3 Sorption isotherm constants and Bayesian information criterion of Freundlich, double Langmuir and Redlich–Peterson isotherm models

Model	Parameter	Zn(II)	Ni(II)
Langmuir	Q^0 , mg/g	61.16	58.29
	b	0.0218	0.0119
	BIC	-3.92	19.55
Double Langmuir	Q_1^0	30.58	29.14
	b_1	0.0218	0.5194
	Q_2^0	26.58	24.14
	b_2	0.0218	0.01194
	BIC	-5.14	-18.82
Dubinin–Radushkevich	β	-0.006	-0.007
	q_m	58.88	56.73
	BIC	2.99	-1.75
	E	9.12	8.45
Redlich–Peterson	KR	0.771	1.446
	αR	0.0349	0.0507
	β	0.8079	0.8289
	BIC	-5.13	-26.44

total energy released in bond making between the concerned cations and IAC, causing the release of extra energy in the form of heat [36]. The positive values of ΔS^0 (J/mol K) involve the increased degree of freedom of Ni(II) and Zn(II) ions in the solution [24].

3.3. Batch sorption design rooted in the equilibrium data

It is quite hard to design correctly the size of sorber and sorption process performance unless all experimental and rate controlling steps data are accessible. Thus, empirical design procedures rooted in sorption equilibrium conditions are the most widespread method for predicting the sorbent amount and performance. The mass balance equation for batch removal system is illustrated in Fig. 9.

Table 4 Thermodynamic parameters for the sorption of Zn(II) and Ni(II) onto IAC

Thermodynamic parameter	ΔH^0 (KJ/mol)	ΔS^0 (J/mol)	Temperature (K)	ΔG^0 (KJ/mol)
Zn(II)	-8.83	46.27	298	-22.59
			303	-23.14
			313	-23.52
Ni(II)	-7.44	51.14	298	-22.68
			308	-23.19
			318	-23.71

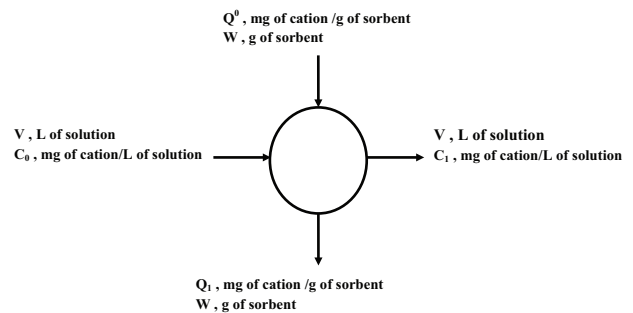


Fig. 9. A single-stage batch sorption process.

Deem that V (L) is the volume of the solution and the cation concentration reduced from C_0 to C_1 mg cation/per L solution. The sorbent amount was m (g) and the cation loading varied from q_0 to q_1 mg cation per g sorbent. The mass balance equates the cation removed from the liquid and picked up by the sorbent. The mass balance equation related to the sorption system can be written as:

$$V(C_0 - C_1) = m(q_0 - q_1) \tag{13}$$

At equilibrium state, the subsequent equation becomes:

$$V \cdot C_0 + m \cdot q_0 = V \cdot C_e + m \cdot q_e \tag{14}$$

It was deduced from equilibrium studies that both Zn(II) and Ni(II) cations removal by IAC followed R–P model. The aforesaid equation can be rearranged as following:

$$\frac{m}{V} = \frac{(C_0 - C_1)}{q_0} = \frac{(C_0 - C_e) \cdot (1 + \alpha_R C_e^\beta)}{K_R C_e} \tag{15}$$

Excluding the 100% elimination conditions, the sorbent dose amount necessitated for the essential percentage removal of the concerned cations from aqueous solution can be calculated via the use of Eq. (15). Fig. 10 shows the series of plots for the sorption of Zn(II) and Ni(II) cations onto IAC and the use of these plots to calculate the optimum quantity required for the treatment of known effluent volume. The amount of IAC required to reduce the final concentration to 75%–95% for different volumes of the solution is shown in Fig. 10.

In case of a single-stage batch sorption system, the design procedure can be now outlined. The results of present investigation showed that the IAC has considerable potential for the removal of cations selected from aqueous solutions over a wide range of concentrations. For instance, the amount of IAC required for the 95% elimination of

Zn(II) and Ni(II) on IAC of concentration 20 mg/L was 112, 225, 336 and 448 mg and 92, 185, 278 and 370 mg for Zn(II) and Ni(II) solution volumes of 100, 200, 300 and 400 mL, respectively.

3.4. Comparative material

Table 5 shows the comparison amid different types of ACs, found in literature, and those of the synthesized IAC. It can be concluded that IAC has a high sorption capacity that can be used for Zn(II) and Ni(II) trapping from aqueous solutions [40–45]. The efficacy of the studied sorbent in the presence of natural water was studied (Fig. 11) and it is observed that the sorbed amount of cations decreased in presence of natural water that due to existence of more competitive ions in natural water.

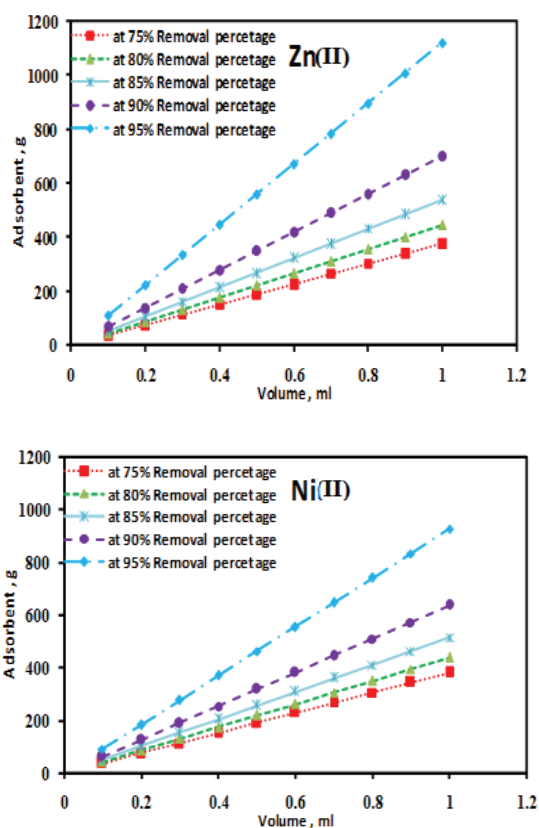


Fig. 10. Sorbent mass (m) against treated effluent volume (V) for different removal percentages of Zn(II) and Ni(II) cations ($C_0 = 20$ mg/L).

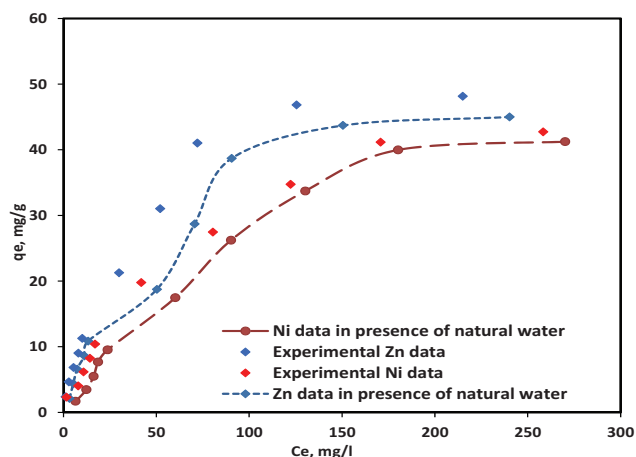


Fig. 11. Equilibrium isotherm for the sorption of Zn(II) and Ni(II) cations onto synthetic IAC in presence and absence of natural water.

Table 5
Comparison between sorbing materials and the synthesized impregnated activated carbon

Sorbing material	Ni ²⁺ , mg/g	Zn ²⁺ , mg/g	References
Rice husk-based activated carbon carbonized at 400°C	2.69	5.28	[40]
600°C	3.88	5.38	
800°C	6.23	6.17	
Sugar cane-based activated carbon	10.03	27.30	[41]
Polystyrene-based activated carbons	20.82	–	[42]
Oil palm and coconut shells-based activated carbons	3.18	–	[43]
Palm shell-based activated carbons using H ₃ PO ₄ impregnated	10.83		
Coconut shell-based activated carbons using H ₃ PO ₄ impregnated	12.18		
Delonix regia ZnCl ₂ activated carbon at 303°C	12.05	–	[44]
313°C	15.38		
Wood-activated carbon	–	20.52	[45]
Impregnated rice husk-based activated carbon	58.29	61.16	Present study

4. Conclusion

The capability of nano-sized IAC to remove Zn(II) and Ni(II) from aqueous solution was investigated. Experimental results illustrate that IAC was effective for the removal of Zn(II) and Ni(II) from aqueous solution. As IAC used in this study is freely, plentifully and locally available, the resulting sorbent is supposed to be economically viable for Zn(II) and Ni(II) removal from aqueous solution. Sorption experiments were performed as a function of contact time, sorbent dose and initial pH of cation solution. The sorption of Zn(II) and Ni(II) could reach equilibrium rapidly at about 60 min and the pseudo-second-order kinetic model precisely described Zn(II) and Ni(II) sorption kinetics by IAC. The sorption acceleration sign in first and second regions was negative and it was observed that the initial sorption velocity increased in increasing time by KASRA model. The data of sorption isotherm agreed well with R-P and dual-site Langmuir models. It was found that the cations sorption on IAC took place in both type I and II sites that varied in both the sorption affinity and maximum sorption capacity. The R_L value can be utilized as the criterion for the cations sorption mechanism assessment as its value in case of Zn(II) and Ni(II) sorption process in type I sites revealed the characteristics of chemical sorption; conversely, in case of type II sites, the characteristics of physical sorption. The obtained AC appeared to be suitable for the removal of Zn(II) and Ni(II) from aqueous solutions. The sorption process of Zn(II) and Ni(II) onto IAC was spontaneous and exothermic in nature. Moreover, the (ΔS°) value indicated an increased randomness at the solid–solution interface during the sorption interaction.

References

- [1] M. Dehghani, D. Sanaei, I. Ali, A. Bhatnagar, Removal of chromium(VI) from aqueous solution using treated waste newspaper as a low-cost adsorbent: kinetic modeling and isotherm studies, *J. Mol. Liq.*, 215 (2016) 671–679.
- [2] B. Alyuz, S. Veli, Kinetics and equilibrium studies for the removal of nickel and zinc from aqueous solutions by ion exchange resins, *J. Hazard. Mater.*, 167 (2009) 482–488.
- [3] F. Fu, Q. Wang, Removal of heavy metal cations from wastewaters: a review, *J. Environ. Manage.*, 92 (2011) 407–418.
- [4] G. Chibuike, S. Obiora, Heavy metal polluted soils: effect on plants and bioremediation methods, *Appl. Environ. Soil Sci.*, 204 (2014) 1–12.
- [5] H. Kalavathy, B. Karthik, L.R. Miranda, Removal and recovery of Ni and Zn from aqueous solution using activated carbon from *Hevea brasiliensis*: batch and column studies, *Colloids Surf., B*, 78 (2010) 291–302.
- [6] H. Kalavathy, L.R. Miranda, *Moringa oleifera*—a solid phase extractant for the removal of copper, nickel and zinc from aqueous solutions, *Chem. Eng. J.*, 158 (2004) 188–199.
- [7] O.A. Abdel Moamen, H.S. Hassan, E.A. El-Sherif, Binary oxide composite adsorbent for copper, nickel and zinc cations removal from aqueous solutions, *Desal. Wat. Treat.*, 82 (2017) 219–233.
- [8] S. Song, A. Lopez-Valdivieso, D.J. Hernandez-Campos, C. Peng, M.G. Monroy-Fernandez, Arsenic removal from high-arsenic water by enhanced coagulation with ferric cations and coarse calcite, *Water Res.*, 40 (2006) 364–372.
- [9] A.M.M. El-Torky, H.Y. Mostafa, A.M.M. El-Masry, M.E. Mahdi, Removal of heavy metals from waste water using amidoximated acrylonitrile grafted corn husks cellulose as an ion exchanger, *Int. J. Adv. Res.*, 3 (2015) 122–139.
- [10] A. Hassan, M. Ariffin, M. Puteh, Pre-treatment of palm oil mill effluent (POME): a comparison study using chitosan and alum, *Malaysian J. Civil Eng.*, 19 (2007) 128–141.
- [11] C. Nguyen, D. Do, Dual Langmuir kinetic model for adsorption in carbon molecular sieve materials, *Langmuir*, 16 (2000) 1868–1941.
- [12] A.M.M. El-Torky, H.Y. Mostafa, A.M.M. El-Masry, M.E. Mahdi, Purification of heavy metals from industrial waste water using grafted corn husks pulp ion exchanger, *Int. J. Adv. Res.*, 3 (2015) 936–949.
- [13] O. Pezoti Jr., A.L. Cazetta, I.P.A.F. Souza, K.C. Bedin, A.C. Martins, T.L. Silva, V.C. Almeida, Sorption studies of methylene blue onto ZnCl₂-activated carbon produced from buriti shells (*Mauritia flexuosa* L.), *J. Ind. Eng. Chem.*, 20 (2014) 4401–4407.
- [14] S.A. Torrellas, R.G. Lovera, N. Escalona, C. Sepúlveda, J.L. Sotelo, J. García, Chemical-activated carbons from peach stones for the adsorption of emerging contaminants in aqueous solutions, *Chem. Eng. J.*, 279 (2015) 788–798.
- [15] J. Shah, M.R. Jan, A.U. Haq, M. Sadia, Adsorptive removal of Ni (II) from aqueous solutions using carbon derived from mulberry wood sawdust, *J. Chem. Soc. Pak.*, 34 (2012) 58–66.
- [16] Y.J. Zhang, J. Ou, K. Duan, J. Xing, Y. Wang, Sorption of Cr(VI) on bamboo bark-based activated carbon in the absence and presence of humic acid, *Colloids Surf. A*, 481 (2015) 108–116.
- [17] A. El-Nemr, O. Abdel-Wahab, A. El-Sikaily, A. Khaled, Use of rice husk for sorption of direct dyes from aqueous solution, *Bull. Nat. Inst. Oceanogr. Fish.*, 31 (2005) 1–12.
- [18] L. Lin, S. Zhai, Z. Xiao, Dye sorption of mesoporous activated carbons produced from NaOH-pretreated rice husks, *Bioresour. Technol.*, 136 (2013) 437–443.
- [19] A.E. Ofomaja, Y.S. Ho, Effect of temperatures and pH on methyl violet biosorption by *Mansonia* wood sawdust, *Bioresour. Technol.*, 99 (2008) 5411–5418.
- [20] D. Singh, R. Kumar, A. Kumar, K.N. Rai, Synthesis and characterization of rice husk silica, silica-carbon composite and H₃PO₄ activated silica, *Cerâmica*, 54 (2008) 203–212.
- [21] M. Akhtar, S. Iqbal, A. Kausar, M.I. Bhangar, M.A. Shaheen, An economically viable method for the removal of selected divalent metal cations from aqueous solutions using activated rice husk, *Colloids Surf., B*, 75 (2010) 149–155.
- [22] S. Somasundaram, K. Sekar, V.K. Gupta, S. Ganesan, Synthesis and characterization of mesoporous activated carbon from rice husk for adsorption of glycine from alcohol-aqueous mixture, *J. Mol. Liq.*, 177 (2013) 416–425.
- [23] Y. Li, X. Ding, Y. Guo, L. Wang, C. Rong, Y. Qu, X. Ma, Z. Wang, A simple and highly effective process for the preparation of activated carbons with high surface area, *Mater. Chem. Phys.*, 127 (2011) 495–500.
- [24] O.A. Abdel Moamen, H.A. Ibrahim, N. Abdelmonem, I.M. Ismail, Thermodynamic analysis for the sorptive removal of cesium and strontium cations onto synthesized magnetic nano zeolite, *Microporous Mesoporous Mater.*, 223 (2016) 187–195.
- [25] M.H. Kurbatov, G.B. Wood, J.D. Kurbatov, Isothermal adsorption of cobalt from dilute solutions, *J. Phys. Chem.*, 55 (1951) 1170–1182.
- [26] F.C. Wu, R.L. Tseng, R.S. Juang, Kinetic modeling of liquid-phase sorption of reactive dyes and metal cations on chitosan, *Water Res.*, 35 (2001) 613–618.
- [27] R.O. Abdel Rahman, O.A. Abdel Moamen, M. Hanafy, N.M. Abdel Monem, Preliminary investigation of zinc transport through zeolite-X barrier: linear isotherm assumption, *Chem. Eng. J.*, 185 (2012) 61–70.
- [28] R. Sivanesan, Sorption of dye from aqueous solution by cashew nut shell: studies on equilibrium isotherm, kinetics and thermodynamics of interactions, *Desalination*, 261 (2010) 52–60.
- [29] P.D. Pathak, S.A. Mandavgane, Preparation and characterization of raw and carbon from banana peel by microwave activation: application in citric acid sorption, *J. Environ. Chem. Eng.*, 3 (2015) 2435–2447.
- [30] J. Shah, M. Rasul Jan, M. Khan, S. Amir, Removal and recovery of cadmium from aqueous solutions using magnetic nanoparticle-modified sawdust: kinetics and adsorption isotherm studies, *Desal. Wat. Treat.*, 57 (2016) 9736–9744.
- [31] J. Shah, M. Rasul Jan, A. ul Haq, M. Zeeshan, Equilibrium, kinetic and thermodynamic studies for sorption of Ni (II) from aqueous solution using formaldehyde treated waste tea leaves, *J. Saudi Chem. Soc.*, 19 (2015) 301–310.

- [32] J. Shah, M. Rasul Jan, A. ul Haq, Removal of lead from aqueous media using carbonized and acid treated orange peel, *Tenside Surfact. Deterg.*, 51 (2014) 240–246.
- [33] A.A. Khan, R.P. Singh, Adsorption thermodynamics of carbofuran on Sn(IV) arsenosilicate in H⁺, Na⁺ and Ca²⁺ forms, *Colloids Surf.*, 24 (1987) 33–42.
- [34] J.W. Biggar, M.W. Cheung, Adsorption of picloram (4-amino-3,5,6-trichloropicolinic acid) on panoche, ephrata, and palouse soils: a thermodynamic approach to the adsorption mechanism, *Soil Sci. Soc. Am. Proc.*, 6 (1973) 37–42.
- [35] S.K. Milonjic, A consideration of the correct calculation of thermodynamic parameters of adsorption, *J. Serb. Chem. Soc.*, 72 (2007) 1363–1367.
- [36] X. Zhou, X. Zhou, The unit problem in the thermodynamic calculation of adsorption using the Langmuir equation, *Chem. Eng. Commun.*, 201 (2014) 1459–1467.
- [37] Y. Liu, Is the free energy change of adsorption correctly calculated, *J. Chem. Eng. Data*, 54 (2009) 1981–1985.
- [38] H. Tran, S. You, A. Bandegharai, H. Chao, Mistakes and inconsistencies regarding adsorption of contaminants from aqueous solutions: a critical review, *Water Res.*, 120 (2017) 88–116.
- [39] S. Canzano, Comment on removal of anionic dye Congo red from aqueous solution by raw pine and acid-treated pine cone powder as adsorbent: equilibrium, thermodynamic, kinetics, mechanism and process design, *Water Res.*, 46 (2012) 4314–4315.
- [40] F. Taha, F. Kiat, S. Shaharun, A. Ramli, Removal of Ni(II), Zn(II) and Pb(II) cations from single metal aqueous solution using activated carbon prepared from rice husk, *Int. J. Environ. Chem. Ecol. Geol. Geophys. Eng.*, 5 (2011) 213–220.
- [41] E.U. Ikhuoria, O.C. Onojie, Binding of nickel and zinc cations with activated carbon prepared from sugar cane fiber (*Saccharum officinarum* L.), *Bull. Chem. Soc. Ethiop.*, 21 (2007) 151–156.
- [42] L. Gonsalvesh, S.P. Marinov, G. Gryglewicz, R. Carleer, J. Yperman, Preparation, characterization and application of polystyrene based activated carbons for Ni(II) removal from aqueous solution, *Fuel Process. Technol.*, 149 (2016) 75–85.
- [43] M. Mokhlesur, M. Adil, M. Yusof, B. Kamaruzzaman, H. Ansary, Removal of heavy metal cations with acid activated carbons derived from oil palm and coconut shells, *Materials*, 7 (2014) 3634–3650.
- [44] I. Rajappa, K. Ramesh, V. Nandhakumar, Adsorption of nickel(II) ion from aqueous solution onto ZnCl₂ activated carbon prepared from *Delonix regia* pods (flame tree), *Int. J. Chem. Phys. Sci.*, 3 (2014) 227–233.
- [45] U. Kouakou, A. Ello, J. Aboua Yapo, A. Trokourey, Adsorption of iron and zinc on commercial activated carbon, *J. Environ. Chem. Ecotoxicol.*, 5 (2013) 168–171.